

# Integrated Optics on Silicon : A MEMS Compatibility

シリコンインテグレートイドオプティクス

Eric BONNOTTE\*, Christophe GORECKI\*, Hiroshi TOSHIYOSHI\*\*,  
Hiroyuki FUJITA\*\* and Hideki KAWAKATSU\*

エリック ボノット・クリストフ ゴレキ・年 吉 洋・藤 田 博 之・川 勝 英 樹

**Abstract** : After a short review of integrated optics, a novel application of Si-based integrated optics and preliminary results of realisation of a compact Mach-Zehnder interferometer will be presented. The deposition of a piezoelectric ZnO thin-film transducer on the reference arm of the interferometer will allow to transform this optically passive device into a device under an active phase modulation, useful to built a high-resolution microsensing systems with optical heterodyning.

**Keywords** : Integrated optics, Micro-interferometry, Surface-acoustic waves, Si-based machining.

## 1. Introduction

The design and realisation of sub-millimetric or micro-metric size devices is a growing field requiring developments in several scientific disciplines. Thus, for the last decade, one can see the merge of a new science called MEMS : Micro Electro-Mechanical Systems. From a general point of view, a MEMS device consists in mechanical structures (microsensor and/or microactuator) and electronic integrated on a same substrat. This results in smart devices. Micromechanical systems are inherently smaller, lighter, faster and more precise than there macroscopic counterparts. Their monolithic nature enhances their reliability. Moreover, one of the main advantages of MEMS device is low cost, due to the batch and IC compatibility processes. The fields of applications are various : automobile, spatial, biomedicine.

## 2. Integrated Optics

Integrated optics (IO) has benefited enormously by the development and fabrication of these microstructures<sup>1</sup> which, in general, are of a physical scale (typically 1 to 200  $\mu\text{m}$ ) that is appropriate for the control of optical radiation. Optical devices

that were considered to be impractical due to the limitations of bulk optics in the 1970s were designed and fabricated easily using micro-optics in the 1980s and IO in the 1990s<sup>2</sup>.

The field of integrated optics is concerned with the theory, fabrication and applications of guided wave optical devices. These devices can be separated in two types : first, passive devices as waveguide bends, polarizers, beam splitters and fiber-to-chip coupling. Second, active devices as modulators or switches. The combination of both passive and active elements in a multicomponent circuit is referred to as an integrated optics circuit (IOC) or a photonic electronic devices can be integrated as well to form an optoelectronic integrated circuit (OEIC). Furthermore, using semiconductors materials and processes allows these devices to be monolithically combined with lasers, detectors and optical amplifiers. Finally, the approach of microsensing based on integrated optics is very attractive because of the insensitivity to electromagnetic noise and, of course, ability for non-contact measurements.

### 2.1 Active devices

The majority of IO R&D from 1975 to 1985 and the most part of the currently commercial active IO components utilise Niobate Lithium ( $\text{LiNbO}_3$ ) as the substrate material<sup>3</sup>.  $\text{LiNbO}_3$  is an excellent electro-optic material with high optical transmission in the visible to near infra-red range, relatively large

\* 2 rd Department, Institute of Industrial Science, University of

\*\* 3 rd Department, Institute of Industrial Science, University of Tokyo

refractive index ( $n = 2.15 - 2.2$ ) and a very large electro-optic coefficient<sup>4</sup>. These high qualities led to use Niobate Lithium mainly in optical communications field, required low losses and high frequencies switching. However, although  $\text{LiNbO}_3$  is a crystalline material, his incompatibility with standard semi-conductor processes is a drastic limitation in MEMS applications<sup>5</sup>.

This is the reason why many research are now focused on new materials, preferably compatible with MEMS technology.

## 2.2 Polymers films

Organic Polymer films are a relatively new class of materials for Integrated Optics<sup>6</sup>. They can be applied by coating techniques to many different substrates and their optical and electro-optical properties can be modified in a variety of ways. Of course, their compatibility with batch processes would dramatically reduce active devices manufacturing cost with respect to Niobate Lithium systems. However, until now, a limitation in the use of polymer films is observed with the decrease of the wavelength of the laser source. As an example, the high electro-optic coefficient at  $1.32 \mu\text{m}$  dropped under 50% at  $0.633 \mu\text{m}$  and dramatically fallen under 17% at  $0.543 \mu\text{m}$ .

If someone wants to build a high-resolution displacement sensor in the visible range, one could see that polymers film are not yet well appropriate.

## 2.3 Thin film oxides

In recent years, there has been substantial interest in IO devices fabricated in thin film dielectric on silicon substrates. This is due in part to the excellent surface quality, large-area wafers, good mechanical properties and integrities of silicon itself. Two fundamental approaches are suitable in order to produce  $\text{Si}/\text{SiO}_2$  high performances IO devices. First is called flame hydrolysis<sup>7</sup> and get out of the frame of this paper. Second, which will be describe later, is the classical thin films deposition technology derived from silicon electronics processing. The biggest disadvantage of this material is his passive character, that means, unfortunately, no electro-optics effect.

## 2.4 Silicon-based Integrated optics Micro-components

Respectively to the previous description of active and passive optical devices, it could be interesting to distinguish different types of thin films oxide IO systems. A first family consists in optical modulators and switches. Micromachined switches offer higher isolation, lower power consumption and the possibility of bistable operation<sup>8</sup>. These advantages, added to the batch fabrication using inexpensive silicon technologies are preponderant for the commercial viability of such devices in a near future.

Many researchers are now working in this direction and a LIMMS project (Figure 1) was devoted to the study of an optical switch using evanescent interactions<sup>9</sup>.

A second group of thin films oxide IO devices is the microsensors area. The principle of an optical microsensor is quite simple : the light is propagated through a waveguide and a interaction that affects the guided light can be utilised as the 'sensitive element'. These interactions can be : amplitude, optical path modulation, phase and polarisation. Using this different kinds of perturbation combining with Mach-Zehnder or Michelson geometry, one can imagine a wide variety of optical microsensors : displacement sensor<sup>10</sup>, accelerometer<sup>11</sup>, pressure and temperature sensor<sup>12</sup>, Chemical and gas sensor<sup>13</sup> but also new type of actuators, as direct optical actuator<sup>14</sup> which converts optical power in mechanical displacement.

In the next chapter, we will see in details a new type of micro-interferometer integrated on silicon, which is a second LIMMS project in the field of IO on silicon.

## 3. Micro-interferometer

### 3.1 Design of integrated device architecture

The proposed Mach-Zehnder microinterferometer architecture is shown in Figure 2. It consists of combined sensing and reference arms composed by two symmetrical Y-junctions integrated on Si substrate using SiON strip-loaded waveguide

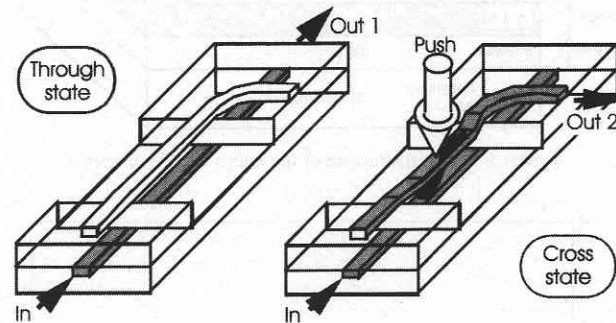


Figure 1 Silicon Electro-mechanical switch

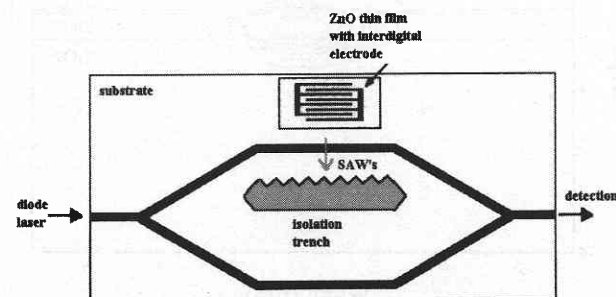


Figure 2 Si-based Mach-Zehnder micro-interferometer

technology<sup>15</sup>. The waveguide structure SiO<sub>2</sub>/SiON/SiO<sub>2</sub>, operating at λ = 660 nm, is shown in **Figure 3**. Since Silicon itself not only has a high refractive index but also absorbs in the visible (imaginary part of the index), it is necessary to isolate the substrate from the waveguide with a low index buffer layer (3 μm of SiO<sub>2</sub> with n = 1.454). The waveguide core is fabricated with a refractive index n = 1.51 and a 0.5 μm thick layer of SiON. SiO<sub>2</sub> rib (width w = 4 μm and n = 1.454) laterally confines the optical field. For an Y-junction of a total length of 24 mm with a gap of 200 μm between measuring and reference arms, the optical field distribution in the output cross-section was calculated by 3D Beam Propagation Method (**Figure 4**). To decrease the losses in the Y-junction both the Y-junction curvatures are of S-bend type based on a cosine function, where the curvature of minimum radius is used to connect the start and end coordinates.

As it says previously, silicon is, from an optical point of view, a passive material. However, in order to increase resolution and accuracy of the micro-interferometer, it is fundamental to imple-

ment an heterodyne technique. This can be achieved in an optical waveguide via phase modulation. Usually, this is obtained by altering the refractive index of the guiding region. The induced grating structure causes diffraction of the guided optical wave, resulting in modulation<sup>16</sup>. In our device, acoustic waves can be used to generate the desired grating pattern in the index profile<sup>17, 18</sup> and we propose to obtain this with a piezoelectric thin film transducer deposited on the silicon waveguide<sup>10</sup>. By use of elasto-optic effect the phase modulation is obtained by passing the guided reference beam through a surface acoustic wave (SAW) induced by a thin-film of ZnO deposited directly on the top of the substrate. Elasto-optic effect produces a grating-shaped variation of the index of refraction within the waveguide caused by mechanical strain which is generated by the passage of an acoustic wave. To avoid perturbations on the measuring arm of the interferometer, acoustic waves have to be confined in the region of the reference arm by an isolation trench (**Figure 5**). Interdigitated metal electrodes are used to launch locally Saw.

For a N-period interdigital transducer the frequency variation of acoustic amplitude can be approximated for frequencies near ω<sub>0</sub> by the function  $\frac{\sin x}{x}$  where  $x = \frac{N\pi(\omega - \omega_0)}{\omega_0}$ . The useful criterion of the transducer performance is the transducer radiation<sup>19, 20</sup> defined as :

$$\frac{1}{Q} = \omega_0 N C_s R_A = N\pi \frac{\Delta v}{v} = \frac{\pi}{2} N K^2 \dots \dots \dots (1)$$

$$\text{with } K^2 = 2 \left( \frac{\Delta v}{v} \right)$$

where ω<sub>0</sub> is the centre-of-band frequency, C<sub>s</sub> is the elementary finger capacitance, k<sup>2</sup> is the electromechanical coupling coefficient, R<sub>A</sub> is the radiation impedance, and Δv is the change in acoustic velocity caused by introducing a short-circuiting

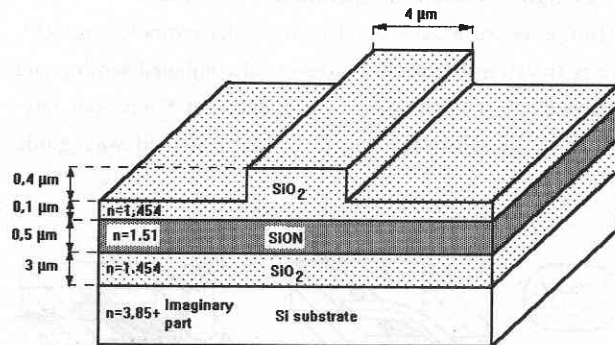


Figure 3 layered structure of the micro-interferometer

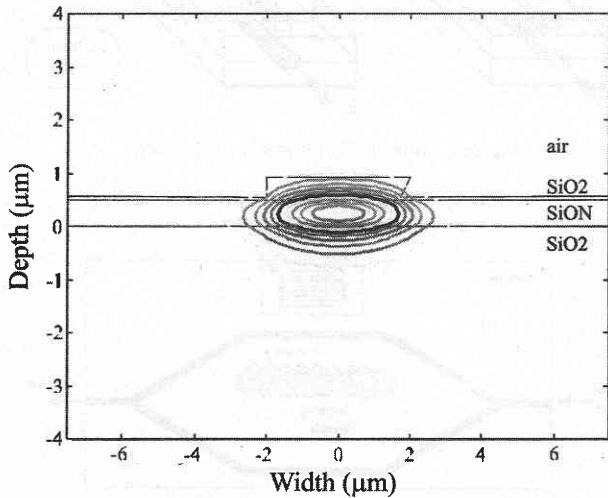


Figure 4 Optical field distribution

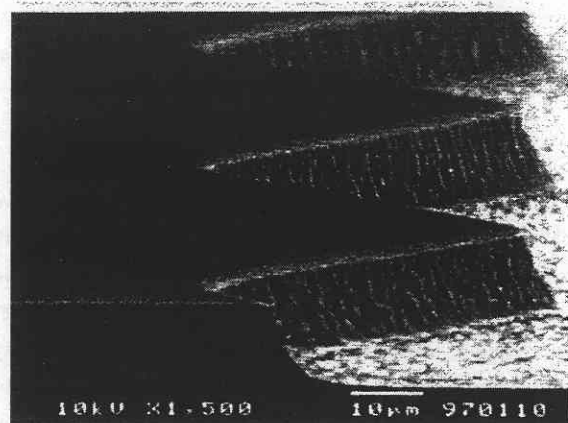


Figure 5 Isolation trench

plane in the plane of interdigital electrode.

Under the condition of using the matching network defined by W.R. Smith<sup>19</sup>, the electronic bandwidth of the system is determined by the product  $\Delta v/v$  and the number  $N$  of finger pairs.  $Q$  is then proportional to  $1/N$  when optimum value of  $N$  is used. The fabricated transducer has an interdigital period of  $60 \mu\text{m}$  (that correspond to a frequency  $f_0 = 48 \text{ MHz}$ ) with a finger width of  $5.8 \mu\text{m}$ . When  $R_A = 75 \Omega$ ,  $C_s = 0.14 \text{ pF}$ , the  $N = 15$  transducers is found to have the optimum fractional bandwidth of 0.08, corresponding to the 3 dB conversion loss ( $1/N$  is 0.067). The theoretical coupling efficiency of a  $2.5 \mu\text{m}$  ZnO film on  $\text{SiO}_2$  layer with 15 finger pairs is about  $k^2 = 0.002$ .

### 3.2 Device fabrication

The interferometer fabrication sequence is shown in **Figure 6**.

3" wafers <100> are used. The process starts by the LPCVD of three layers  $\text{SiO}_2/\text{SiON}/\text{SiO}_2$ .  $\text{SiON}$  and  $\text{SiO}_2$  layers are deposited in a temperature range of  $600\text{--}850^\circ\text{C}$  by appropriate adjusting of the gas flow of the  $\text{SiH}_4/\text{O}_2$  mixture and of the  $\text{SiH}_4/\text{N}_2\text{O}/\text{NH}_3$  gases. The top  $\text{SiO}_2$  layer is etched by RIE to

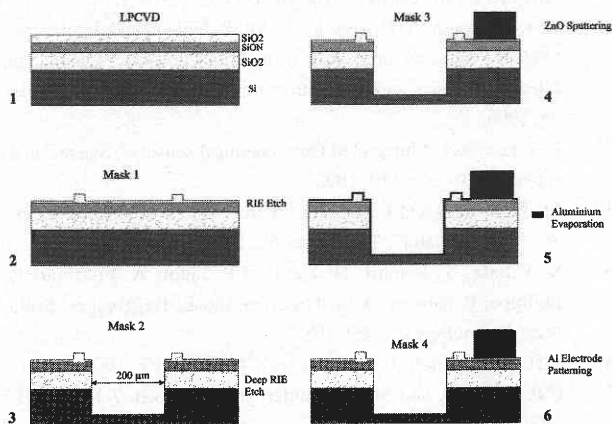


Figure 6 Fabrication process

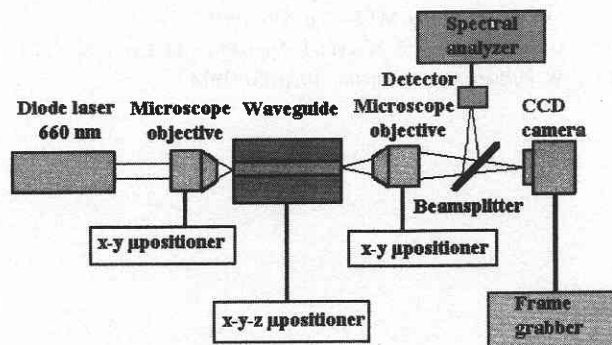


Figure 7 Experimental setup

form the rib structure of strip-load optical waveguide. To pattern the isolation grooves a deep RIE etching is used.

ZnO thin film is deposited by DC magnetron sputtering directly on the top of the  $\text{SiO}_2$  layer near the rib. To pattern the interdigital electrodes a thin film of Al is deposited by vacuum evaporation on the front surface of the wafer. The metal layer is subsequently wet etched to pattern the structure of the upper transducer electrode.

### 3.3 Experimental results

To evaluate the optical performances, a diode laser beam operating at  $660 \text{ nm}$  was coupled via a microscope objective into the Mach-Zehnder input (**Figure 7**). An intrinsic waveguide loss of roughly  $4 \text{ dB/cm}$  was measured in the straight sections of the waveguide. The maximum spot size of the guided mode estimated to be about  $6.5 \mu\text{m}$  (**Figure 4**) is much smaller than SAW wavelength of  $60 \mu\text{m}$ . In this condition, there is no diffraction and the guided optical wave is only sinusoidally phase modulated.

Modulation experiment was demonstrated by detecting the spectrum of the interference signal via a spectre analyser, as shown in **figure 8**. As expected, there is a component according to the SAW frequency  $f_0 = 48 \text{ MHz}$  (first harmonic). The second and third harmonics also appear frequency spaced<sup>21</sup> by  $f_0$ . From the detected ratio of the first to third harmonic, it is possible to estimate the phase shift: the amplitude of the third harmonic is about  $20 \log[J_1(\delta\phi)/J_3(\delta\phi)] = 31 \text{ dB}$  below the first harmonic, with  $J_{i=1,3}$  the Bessel functions. According this,  $J_1(\delta\phi)/J_3(\delta\phi) = 36.15$  and the phase shift is around  $0.8 \text{ rad}$ .

### 4. Conclusions

After a brief review of IO, we have presented the design and analysis of a strip-loaded-waveguide-based silicon microinterferometer with phase modulation by elasto-optic effect. This device has a very low operating power requirement. The main reason for choosing a multilayered waveguide is that this struc-

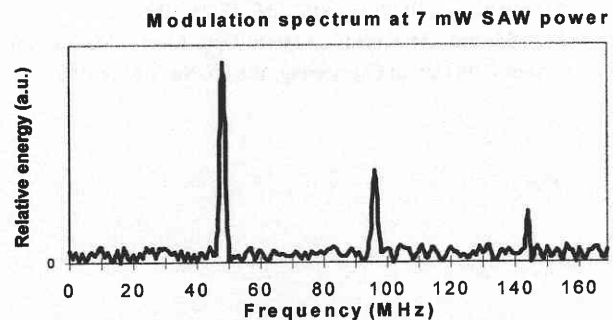


Figure 8 Modulation spectrum at 7 mW SAW power

ture offers a flexible tool for design the better optical architecture needed to increase the efficiency of acousto-optic interactions. Thus, the refractive index of the guided mode can be chosen within a range from 1.5 to 2, which offers a great freedom in the definition of the optimal planar technology. Furthermore, the Si-based technology provides a natural solution to machining a fibre guiding grooves for coupling light source and integrated photodiodes by silicon bonding. This device, fabricated by IC standard equipment (LPCVD, RIE, Sputtering) is CMOS compatible.

The electro-mechanical coefficient  $k^2$  can be easily adjusted by the modification of both piezoelectric film thickness and interdigital electrodes configuration.

We demonstrated that a such device can work on a non-electro-optics substrate if a piezoelectric transducer is utilised to excite SAW. A single one SAW can modulate many waveguides without any electrode rearrangements or additional acoustic power. This is only limited by the propagation loss of SAW.

Beside these advantages, the integrated device shows some disadvantages. Acoustic losses are significant with ZnO on silicon structure and they become drastic at high frequency. Additional losses are due to the presence of bulk waves excited by the film transducer. Many improvements will be achieved on this first device in the optical and acoustic fields.

The future application of the device will be in the sensor area and especially in high resolution displacements measurement.

#### Acknowledgement

The authors would like to express their thanks to the Canon Foundation in Europe and the JSPS in JAPAN for supporting this work.

(Manuscript received, September 26, 1997)

#### References

- 1) S. W. Smith, M. Mehregany, F. L. Merat and D. A. Smith: "All-silicon waveguide and bulk-etched alignment structure on (110) silicon for integrated MOEMS", in Integrated Optics and Microstructures III, Proc. SPIE 2686, 17-28, 1996.
- 2) M. Edward Motamedi: "Micro-Opto-Electro-Mechanical Systems", in Optical Engineering, Vol. 36, No. 5, May 1997.
- 3) T. L. Koch, F. J. Leonberger and P. G. Suchoski in "Handbook of Optics", Chapt. 6, 6.1-6.42, 1995.
- 4) E. Voges and A. Neyer: "Integrated optics devices on LiNbO3 for optical communication", J. Lightwave Technology, LT-5 (9), 1229-1238, 1987.
- 5) Y. Shi and al. in Applied Physics Letters 70 (11), 1342, March 1997.
- 6) E. V. Tomme, P. P. Van Deale R. G. Baets and P. E. Lagasse: "Integrated optics devices based on non-linear optical polymers", IEEE J. Quantum Electron., Vol. QE-27, p. 778, 1991.
- 7) M. Kawachi: "Silica waveguides on silicon and their applications to Integrated optic components", Opt. And Quantum Electron., 22, 391-416, 1990.
- 8) L. A. Field, D. L. Burrieci, P. R. Robrish and R. C. Ruby: "Micromachined 1 x 2 optical-fiber switch", Sensors and actuators A53, 311-315, 1996.
- 9) F. Chollet, M. de Labachellerie, H. Fujita: "Micro-opto-Mechanical devices: an electrostatically actuated bending waveguide for optical coupling", in Micro-optical technologies for measurements, sensors and microsystems, Proc. IEEE 2783, 163-173, 1996.
- 10) C. Gorecki, F. Chollet, E. Bonnotte, H. Kawakatsu: "Silicon-based integrated interferometer with phase modulation driven by acoustic surface waves", December 1977, vol 22, No. 23, optics letters.
- 11) K. E. Burcham, G. N. de Bradander and J. T. Boyd: "Micromachined silicon cantilever beam accelerometer incorporating an IO waveguide", Proc. SPIE 1793, 12-18, 1992.
- 102) O. K. Mawardi, S. Pelkowski, J. Wu, P. Jenkins and Tabib-azar: "Velocity and pressure sensor using GaAs geodesic sensors", in Integrated Optics and Microstructures III, Proc. SPIE 2686, 29-36, 1996.
- 13) P. V. Lambeck: "Integrated Opto-chemical sensors", Sensors and actuators, B8, 103-116, 1992.
- 14) M. Tabib-Azar and J. S. Leane: "Direct optical control for a silicon micro-actuator", Transducer'89, 1989.
- 15) S. Valette, S. Renard, H. Denis, J.P. Jadot, A. Fournier, P. Philippe, P. Guidon, A.M. Grouillet and E. Desgranges, Solid State Technology 2, p. 69, 1989.
- 16) C.H. Von Helmolt, J. of Light. Tech. LT-5, p. 218, 1987.
- 17) C.P. Sandbank and M.B.N. Butler, Electron. Lett. 7-17, p. 501, 1971.
- 18) F.S. Hickernell, J. Appl. Phys. 44-3, p. 1061, 1973.
- 19) W.R. Smith, H.M. Gerard, J.H. Collins, T.M. Reeder and H.J. Shaw, IEEE Trans. MTT-17, p. 856, 1969.
- 20) G. S. Kino and R. S. Wagers, J. Appl. Phys. 44-4, p. 1480, 1973.
- 21) W. Pushert: Opt. Commun., 10, p 357, 1974.